

Preparation and Characterization of PPY/BaFe_(12-x)Ti_xO₁₉ Nanocomposite

Aparna. A. R¹

¹Department of Nanoscience & Technology,
JNTUH, India,

Dr. Brahmajirao.V²

²Department of Nanoscience and Technology,
GVPCE (Autonomous),
Madhurawada, Visakhapatnam, India

Dr. Kartikeyan.T.V³

³Department of Mechanical Engineering,
ASL, India Email:

Abstract— The preparation of hybrid composite in two stages is being presented in this paper. There are two stages of synthesis. In first stage, Ti-doped barium ferrite powders BaFe_(12-x)Ti_xO₁₉ (for x = 0.33 and 0.37) nanomaterial using sol-gel route were synthesized. In second stage, Ti-doped barium ferrite powders BaFe_(12-x)Ti_xO₁₉ nanomaterial synthesized in the first stage is incorporated into the Polypyrrole through solution processing method. The phase structure and morphology were analyzed by standard XRD, SEM, EDS and FTIR techniques. TEM and SAED were done on Nanocomposite samples to know the dispersion of PPY with BFTO nanopowder. Scifinder software couldn't trace any earlier communication involving this nanomaterial in literature.

Keywords— Barium ferrite, sol-gel route, Titanium, Nano ferrite, impregnation technique)

I. INTRODUCTION

Barium ferrite (BaFe₁₂O₁₉) is a permanent magnetic material, a ferrimagnetic material better chemical stability, High saturation magnetization, great coercivity and it is a low cost material.

It has a very wide range of application, very useful in Microwave communication, useful in microwave dark room, absorber for electromagnetic wave radiation (microwave absorbing materials reduce the human exposure to microwaves by means of absorbing coatings) [1-3]

Barium ferrite has hexagonal structure. It belongs to magneto-plumbite ceramic oxide group and can be classified as hard magnetic material. It is one of a ferromagnetic oxide that has both dielectric and magnetic properties when applied with high frequency (microwave region), hence is ideal for microwave applications. The Fe³⁺ ions occupy the sub lattice at different sites that lead to different magnetic properties and change its sub lattice and magnetic properties on addition of nonmagnetic materials [4-6].

Ti-doped barium hexaferrite (Ti-doped BHF) powder is an efficient absorber of electromagnetic waves in the microwave spectrum increase in the saturation magnetization (M_S) and a decrease in the coercivity (H_C) are required for optimization of the absorption. These properties depend on the localization of the Ti₄₊ in the barium hexaferrite structure. The Ti₄₊ ions preferentially occupy the octahedral 4f₂ sites of the BHF structure when the Ti-doped BHF is synthesized using the sol-gel route, especially at low doping rates. Also Since the magnetic moment of the Ti₄₊ ions is zero and the spin direction of 4f₂ site in the BHF structure is down. M_S must increase with the doping concentration of titanium, while H_C must decrease, which corresponds our expectations of lower magnetocrystalline anisotropy. However with higher doping rates of Ti₄₊, M_S decreases, because Ti₄₊ ions could be located also in other lattice sites [7-12].

Both polyaniline (PANI) and polypyrrole (PPy) are Probably the most widely studied conducting polymers due to their good stability in air, high conductivity, and reversible process between oxidation and reduction state. Polypyrrole can be dispersed into metallic fillers like Ferrites by easy methods [13-25].

II. EXPERIMENTAL METHOD

Ti doped barium ferrite was prepared by Sol-Gel method. BaFe_{11.67}Ti_{0.33}O₁₉ and BaFe_{11.63}Ti_{0.37}O₁₉ at 950°C. The synthesis of Nanoferrite composites was done by Impregnation Technique. The Nanoparticle impregnation process involves dissolving an appropriate metallic precursor in a polymer and then exposing the substrate to the solution. And reduced by variety of methods resulting in films, powders. This technique has allowed both highly dispersed and uniformly distributed metal nanoparticles and formation of agglomerated clusters of nanoparticles. Substances impregnated into Polymers are generally Dyes, Fragrances, Metal nanoparticles etc.

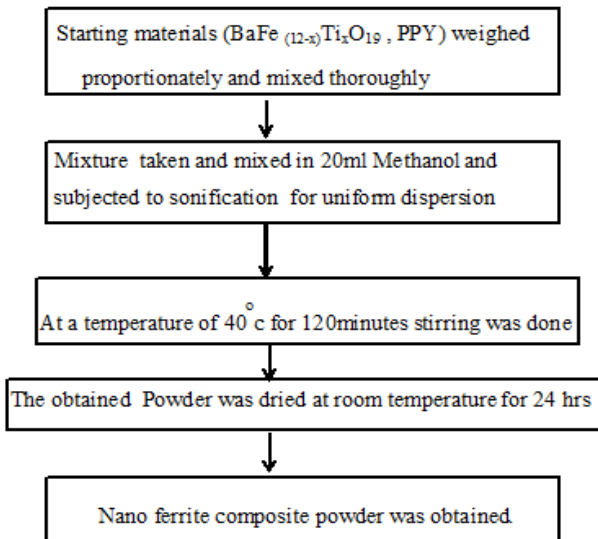


Fig 1. Flow chart for nanoferrite composite preparation

III. RESULTS AND DISCUSSION

A. XRD (X-ray Diffractometer)

XRD was performed at room temperature using CuK α radiation of wavelength 1.5406Å to confirm crystallographic phase formation of nanocomposite material.

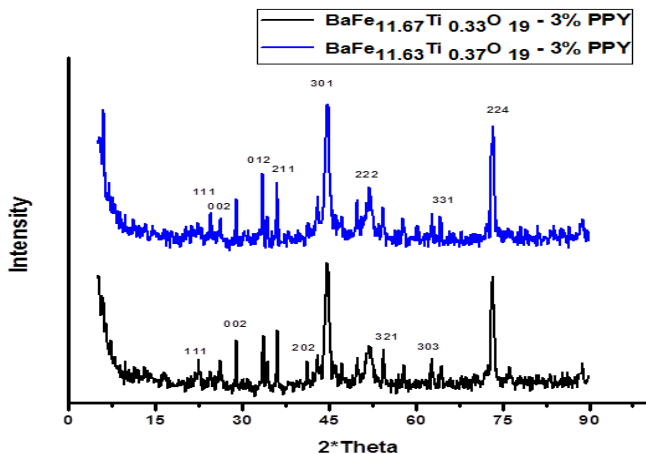


Fig 2. XRD graphs of PPY/Ti-doped barim ferrite for x=0.33 and 0.37 at 950 °C temperatures.

The substituted samples are completely be dissolved in the magneto plumbite lattice and no intermediate phases in the hexagonal plane of magneto plumbite structure are observed. Analyzing the effect of varying the ‘x’ value, we can observe from figure 2 that the sample 2 shows well developed narrow peaks than the sample 1 which indicates that formation of nanoparticles are good at higher ‘x’ value.

Table1. XRD parameters of Nanoferrite Composites at ‘x’ =0.33 and 0.37

S.no	Name of Sample	Crystallite Size “D” nm	Parameter “a” Å	Interplanar Spacing “d” Å	Volume of unit cell gm/cm ³	Density of Unit Cell
1	BaFe _{11.67} Ti _{0.33} O ₁₉ -3% PPY	(11.91)	6.2965	2.01894	249.919	7.7809
2	BaFe _{11.63} Ti _{0.37} O ₁₉ -3% PPY	(13.168)	6.32899	2.4471	254.364	7.78052

The values of the lattice constants, crystallite size,, miller planes determining the type of lattice formed, we found that the prepared doped nanoferrite is a cubic lattice. To know the structural formation of Nanocomposites, XRD technique is done on the samples. We know that PPY is amorphous in nature. By relative comparison of two samples, we can see in the case of sample 1 the interaction of PPY with BaFe_{12-x}Ti_xO₁₉ decreased the average interparticle distance leading to the reduction in the size of Nanoparticles. Varied doping concentration may be the reason for this.

B. SEM(Scanning electron microscopy) and EDAX(Energy dispersive analysis)

The surface morphology of the composite sample was examined using SEM.

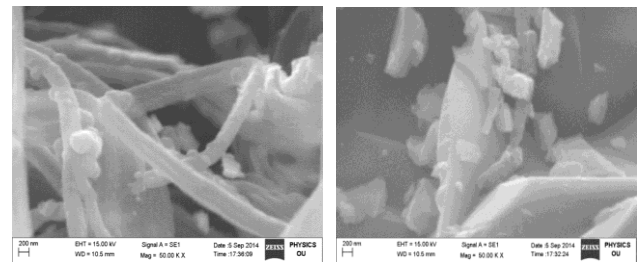


Fig. 3. SEM microgram of PPY/Ti-doped barim ferrite for x=0.33 and 0.37 at 950 °C temperatures

SEM microgram reveals that in sample 1 long and continuous nanorods are more prominent when compared with sample 2, here and there some cubic structure are also present. Whereas in sample 2 short nanorods and cubic structures are present.

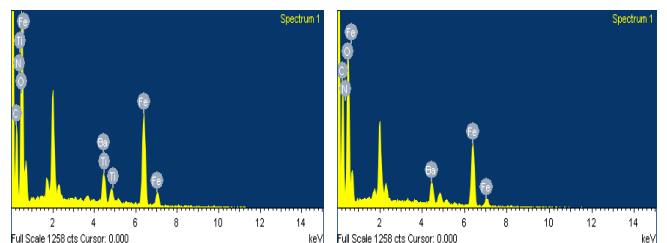


Fig 4.EDAX plots of PPY/Ti-doped barim ferrite for x=0.33 and 0.37 at 950 °C temperatures

EDAX characterization was done in order to ratify the purity and surety of chemical composition. It is a supplementary technique to TEM. The energy dispersive x-ray analysis pattern reveals that these nanoparticles are well crystallized.

In sample 1 ions are present in higher and lower energy levels. This confirms that A-O-B spinel sub-lattice formation. In sample 2 Ti peak at 5Kev energy value are absent, indicating that they were knocked out from lower energy spinel state. Whereas Fe peak at 6Kev has reduced indicating that number of nanoparticles are reduced at that particular energy level. This sample therefore cannot provide absorbing ions for the EMI radiation. Hence their ability for EMI absorption is less. However the above absorption of the Ti ion are necessarily to be confirmed by XPS and mausbaur studies.

C. FTIR (Fourier Transform Infra-Red)

FTIR spectra of the obtained powder were recorded using FTIR spectrometer in the wavenumber range 4000-400cm⁻¹ using kbr pellet to ratify the structure of sample. The identities, surrounding environments and concentration of chemical bonds that are present can be determined.

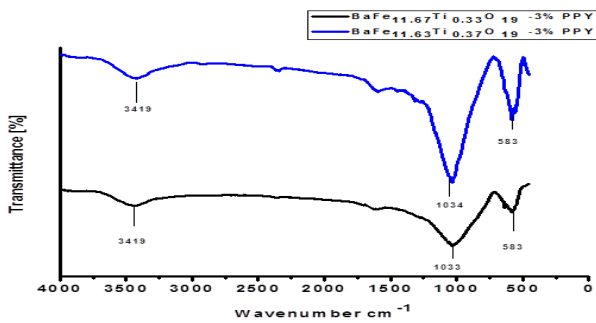


Fig 5. FT-IR spectra of PPy/Ti-doped barim ferrite for x=0.33 and 0.37 at 950 °C temperatures

Dips indicate the formation of groups. The bands around 500cm⁻¹ correspond to metal-oxygen vibration. The bands around 1033, 1034 cm⁻¹ correspond to =C-H band in plane vibration. The peaks around 3000 cm⁻¹ assigned to N-H stretching vibration from pyrrole. Charge carrier existence is confirmed by several peaks indicating bi-polaron band formation. This indicates the formation of PPY in oxidised state.

D. TEM (Transmission electron microscope) AND Histogramic analysis

TEM and SAED were done on Nanocomposite samples to know the dispersion of PPY with BaFe_{12-x}Ti_xO₁₉

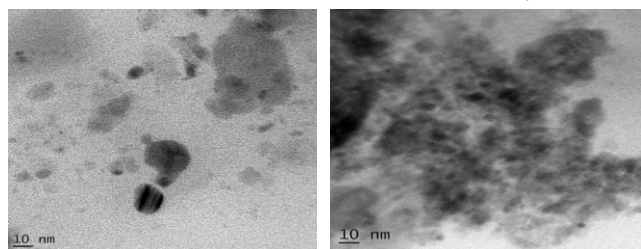


Fig 6. TEM microgram of PPy/Ti-doped barim ferrite for x=0.33 and 0.37 at 950 °C temperatures

In TEM images of BaFe_{12-x}Ti_xO₁₉ for all X-Values studied, the particles appear to be dark. Since ferrite is magnetic in nature, it absorbs more electrons than Ti. Hence appear darker. In BaFe_{12-x}Ti_xO₁₉/PPY, for different percentages of 'x' value the BaFe_{12-x}Ti_xO₁₉ particles are surrounded by PPY confirming the coating of the former by later. In microgram polymer grains are white in colour and Ferrite grains are black in colour. This clearly indicates the formation of core-shell structure with doped ferrite as core and PPY as shell. It is observed that PPY was coated on BaFe_{12-x}Ti_xO₁₉. But for some samples the coating shell obstructed the contact between the rest of PPY and BaFe_{12-x}Ti_xO₁₉. Rest of PPY assembled as oxidant.

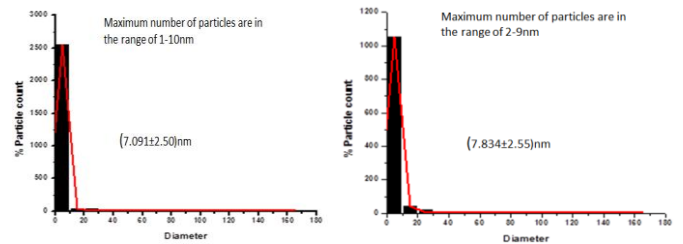


Fig7. Histograms of PPy/Ti-doped barim ferrite for x=0.33 and 0.37 at 950 °C temperatures

Using image j software with SEM and TEM images number of particles distributed size wise are determined. The data is presented as histograms, Gaussian distribution curve is also superimposed to analyse the data. The particle diameter data for the different values of 'X' (calculated using image j software) registered a vivid contrast with similar data from XRD. In general majority of the values of the crystallite parameter D showed reasonably good concurrent with the corresponding parameter of xrd calculations with large values of beta in debye-scherrer equation. The data in (a) TEM and EDX as well as (b) Debye-Scherrer equation from XRD. show reasonably good agreement.

E. SAED (Selected area electron diffraction)

Electron diffraction analysis was used considerably to gain structural information of the sample. Often both electron microscopy (information in real space) images and diffraction patterns (information in reciprocal space) are obtained for the same reason. Electron diffraction can be performed on a single nanoparticle or on an area consisting of multiple nanoparticle, by inserting the relevant selected area aperture. Hence selected area electron diffraction (SAED).

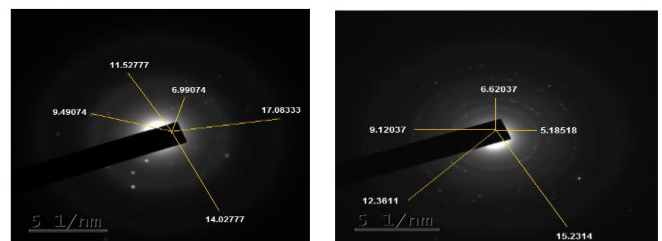


Fig 8. SAED pattern of PPy/Ti-doped barim ferrite for x=0.33 and 0.37 at 950 °C temperatures

Central part is called nose. It is a source of electrons causing diffraction. Bright spots indicate crystalline structure and rings indicate polycrystalline structure. Each bright spot reveals the location of an atom in the crystal. Rings are formed when an atom in a crystal are systematically arranged in different miller plane. If multiple rings are formed more number of miller planes. Such a crystal gives interesting information about interactions with magnetic field, electric field, optical field etc. Sample 2 shows well developed distinct rings indicating polycrystalline structure. Diffraction rings and also Bright spots (in good number) are seen indicating perfect formation of Nanostate .

CONCLUSION

we have successfully incorporated Ti- doped barium ferrite ($x=0.33$ and 0.37) nanopowder into polypyrrolle nanocomposite. The formation of PPy/Titanium doped Nano ferrites has been con-firmed by XRD, SEM studies. FT-IR, EDAX, TEM and SAED studies on the same are also reported.

ACKNOWLEDGMENT

Authors are thankful to the DST SAIF, IIT Madras, department of physics Osmania university, Hyderabad, sophisticated analytical instrumental facility, Cochin for their help to carry out the characterization of samples.

REFERENCES

- [1] Mu G, Pan X, Chen N, He C, Gu M, Synthesis and characterization of hard magnetic composites-Hollow microsphere/titania/barium ferrite, *Appl. Surf. Sci.* 254(2008) 2483-2486.
- [2] Wang C, Han X, Xu P, Wang X, Li X,Zhao H, Magnetic and dielectric properties of barium titanate-coated barium ferrite. *J. Alloy Compd.* 476(2009) 560-565.
- [3] Li Y, Wang Q, Yang H . Synthesis, characterization and magnetic properties on nanocrystalline BaFe12O19. *Curr. Appl. Phys.* 9(2009) 1375-1380.
- [4] Mishra D, Anand S, Panda R K, Das R P, Studied on characterization, microstructures and magnetic properties nano-size barium hexa-ferrite prepared through a hydrothermal precipitation-calcination route. *Mater. Chem. Phys.*86(2004) 132-136.
- [5] Mallick KK, Shepherd P , Green R J, Dielectric properties of M-type barium hexaferrite prepared by co-precipitation. *J. Eur. Ceram. Soc.* 27(2007) 2045-2052.
- [6] Qui J, Lan L, Zhang H, Gu M, Effect of titanium dioxide on microwave absorption properties of barium ferrite. *J. Alloy Compd.* 453(2008) 261-264
- [7] Ruan. S.P, Xu.B.K.,Suo H, Wu. F.Q, Xiang.S.Q, Microwave absorptive behavior of ZnCo-substituted W-type Ba hexaferrite nanocrystalline composite material, *J. Magn. Magn.Mater.* 212(2000) 175-177.
- [8] Halbedel, B., Hülsenberg, D., Belau, St., Schadewald, U.,Synthese und Anwendungen von maßgeschneiderten BaFe12-2xAlIxBiVxO19-Pulvern,*Ceramic Forum International* 82(13) (2005) 182-188 .
- [9] Rohde & Schwarz. A new dimension in compactness.*News* 199/09. 2009, p. 70-72.
- [10] Marino Castellanos.P.A, AngladaRivera.J, Cruz Fuentes. A, Lora Serrano. R.Magnetic and microstructural properties of the Ti4+-doped Barium hexaferrite, *J. Magn.Magn. Mater.* 280(2004) 214-220.

- [11] Brabers.V.A.M, Stevens. A.A.E, Dalderop.J.H.J, Singa.Z,Magnetization and magnetic anisotropy of BaFe12 - xTixO19hexaferrites, *J. Magn.Magn.Mater.*, 196- 197(1999) 312-314.
- [12] Quiroz, P., Halbedel, B., Bustamante, A. et al. , Effect of titanium ion substitution in the barium hexaferrite studied by Mössbauer spectroscopy and X-ray diffraction,*Hyperfine Interact* 202 (2011) 97-106
- [13] Anuar. K, Murali. S, Fariz. A, Ekramul H. N. M,Conducting Polymer / Clay Composites: Preparation and Characterization*Materials Science* 10 (2004) 255-258
- [14] Alexandre. M, Beyer. G, Henrist.C, Cloots. R, Rulmant. A, Jerome. R, Dubois.P, Preparation and properties of layered silicate nanocomposites based on ethylene vinyl acetate copolymers , *Macromolecular rapid communications*, 22(2001) 643-646.
- [15] Rong. J, Jing. Z, Li. H, Sheng. M, A Polyethylene Nanocomposite Prepared via In-Situ Polymerization *Macromol Rapid Commun.*22(2001) 329-334.
- [16] Lim.S.T, Hyun.Y.H, Choi.H.J, Jhon. M.S, Synthetic Biodegradable Aliphatic Polyester/Montmorillonite Nanocomposites , *Chem. Mater* 14(2002) 1839-1844.
- [17] Reichert.P, Hoffmann. B, Bock. T, Thomann. R, Mulhaupt. R,Friedrich.C, Morphological stability of poly(propylene) nanocomposites,*Macromol. Rapid Commun*22 (2001) 519-523.
- [18] Tong X, Zhao H, Tang T, Feng Z and Huang B, Preparation and characterization of poly(ethyl acrylate)/bentonite nanocomposites by in situemulsion polymerization, *J. Polym. Sci. Part A: Polym. Chem*40(2002) 1706-1711.
- [19] Lim. S. K, Kim. J. W, Chin.I, Kwon. Y.K ,Choi. H, Preparation and Interaction Characteristics of Organically Modified Montmorillonite Nanocomposite with Miscible Polymer Blend of Poly(Ethylene Oxide) and Poly(Methyl Methacrylate) .*J. Chem. Mater* 14 (2002) 1989-1994.
- [20] Kim. J. W, Liu.F, Choi. H. J, Hong .S. H, Joo. J,Intercalated polypyrrolle/Na+-montmorillonite nanocomposite via an inverted emulsion pathway method,*Polymer* 44 (2003) 289-293.
- [21] Bianchi. R. F, Onmori. R. K,Faria. R. M,Device model for poly(*o*-methoxyaniline) field-effect transistor ,*J. Polym. Sci. Pol. Phys.* 43 (2005) 74-78.
- [22] Gustafsson. G, Cao. Y, Treacy. G. M, Klavetter. F, Colaneri. N,Heeger.A. J, Flexible light-emitting diodes made from soluble conducting polymers,*Nature.* 357 (1992) 477-479
- [23] Pan T. M, Yeh. W.W,High-Performance High-K Y2O3 SONOS-Type Flash Memory*IEEE Transactions on Electron Devices* 55 (2008) 2354 - 2360.
- [24] Maliakal.A, Katz.H, Cotts.P.M ,Subramoney.S ,Mirau. P,Inorganic Oxide Core, Polymer Shell Nanocomposite as a High K Gate Dielectric for Flexible Electronics Applications,*J. Am. Chem.Soc.* 127 (2005), 14655-14662
- [25] Rao.Y, Yue.J, Wong. C. P, Material Characterization of High Dielectric Constant Polymer-Ceramic Composite for Embedded Capacitor to RF Application*Active and Passive Elec Comp* 25(2002)123-129